Membrane Topology of P-Glycoprotein As Determined by Epitope Insertion: Transmembrane Organization of the N-Terminal Domain of *mdr3*†

Christina Kast,‡ Victor Canfield,§ Robert Levenson,§ and Philippe Gros*,‡

Department of Biochemistry, McGill University, 3655 Drummond Street, Montreal, Quebec, Canada H3G 1Y6, and Department of Pharmacology, Penn State College of Medicine, Milton S. Hershey Medical Center, 500 University Drive, Hershey, Pennsylvania 17033

Received November 28, 1994; Revised Manuscript Received January 19, 1995®

ABSTRACT: P-Glycoproteins (P-gps) are membrane glycoproteins encoded by the *mdr* gene family, and their overexpression is associated with multidrug resistance (MDR). Sequence analyses of *mdr* cDNAs predict a protein formed by two symmetrical halves, each composed of six transmembrane (TM) segments and one ATP-binding domain. To determine the topology of the N-terminal half of P-gp, a small antigenic peptide epitope (YPYDVPDYAIEGR) containing part of the hemagglutinin (HA) of influenza virus was inserted at six different positions of the Mdr3 protein (101, 161, 206, 244, 320, and 376). Functional integrity of the modified proteins was tested by measuring their capacity to confer MDR in Chinese hamster ovary cells. Intracellular and extracellular localization of the tag in the full-length protein was determined in intact or permeabilized cells by immunofluorescence using a mouse monoclonal antibody (12CA5) specific for the HA epitope. While insertions at positions 101, 161, 320, and 376 did not alter P-gp function, insertions at positions 206 and 244 abrogated the capacity of P-gp to confer drug resistance. The epitope tags inserted at positions 161 and 376 were found to be located intracellularly, whereas the tags at positions 101 and 320 were located on the extracellular side of the membrane. These results indicate that the intervening segments separating predicted TM1−TM2 and TM5−TM6 correspond to extracellular regions, while the segments linking TM2−TM3 and the one located downstream of TM6 correspond to intracellular regions. These results are consistent with a six TM domain model for the N-terminal half of P-gp with an extracellular glycosylated region (TM1−TM2) and an intracellular ATP-binding site (downstream TM6). Epitope insertion in segments linking TM3−TM4 and TM4−TM5 caused a loss of P-gp function, suggesting that the integrity of these sequences is essential either for drug transport or for proper maturation and accurate targeting of P-gp to the plasma membrane.

Multidrug resistance in tumor cells *in vivo* and cultured cells *in vitro* is caused by the overexpression of P-glycoprotein (P-gp) (Gottesman & Pastan, 1993). P-gps encoded by human *MDR1* and mouse *mdr1* and *mdr3* have been shown to directly convey MDR (Chen et al., 1986a; Gros et al., 1986; Devault & Gros, 1990), while those encoded by human *MDR2* and mouse *mdr2* cannot (Schinkel et al., 1991; Gros et al., 1988). P-gps are integral membrane phosphoglycoproteins which can directly bind photoactivatable analogs of ATP (Cornwell et al., 1987; Schurr et al., 1989) and drug molecules (Cornwell et al., 1986; Safa et al., 1986, 1993) and have demonstrated ATPase activity [reviewed by Shapiro and Ling (1994)]. Although the mechanism of action of P-gp remains unclear (Valverde et al., 1992; Roepe et al., 1993; Abraham et al., 1993), P-gp appears to use the energy of ATP hydrolysis to reduce intracellular drug accumulation through an active efflux mechanism (Gottesman & Pastan, 1993; Ruetz & Gros, 1994). Sequence analysis of *mdr* cDNA clones predicts a symmetrical protein composed of two sequence homologous halves. Each half contains a hydrophobic region with a potential of forming six transmembrane (TM) domains, and a hydrophilic domain containing consensus sequences for nucleotide binding (NB) (Chen et al., 1986a; Gros et al., 1986). The 6 TM domains/1 NB site structural unit has been preserved through evolution in a large number of membrane-associated transport systems that together form the ABC (ATP-Binding Cassette) superfamily of transport proteins [reviewed by Higgins et al. (1992)]. In *Escherichia coli* and *Salmonella typhimurium*, this group of proteins is known as periplasmic permeases, and includes high-affinity import systems for sugars, amino acids, peptides, and phosphates, and export systems for several toxins, such as hemolysin (*HlyB*; Felmlee et al., 1985). In prokaryotes, the 6 TM domains/1 NB site unit either can be encoded by independent peptides (*PstA*//*PstB*; Surin et al., 1985) or is found fused in different combination within the same peptide (*HlyB*, *ArsA*; Felmlee et al., 1985; Chen et al., 1986b). In lower eukaryotes, the ABC superfamily is examplified by the *STE6* gene of the yeast *Saccharomyces cerevisiae* which transports the "a" mating pheromone (McGrath & Varshavsky, 1989), and the *pfmdr1* gene of *Plasmodium falciparum* associated with chloroquine resistance in the malarial parasite (Foote

† This work was supported by grants to P.G. from the Medical Research Council and the National Cancer Institute of Canada, and to R.L. from the National Institutes of Health. C.K. is supported by a scholarship from the Swiss National Science Foundation, and P.G. by an E.W.R. Steacie Fellowship from the Natural Sciences and Engineering Research Council of Canada. P.G. is an International Research Scholar of the Howard Hughes Medical Institute.

* To whom correspondence should be addressed. Phone: 514-398-7291. FAX: 514-398-2603.

‡ McGill University.

§ Milton S. Hershey Medical Center.

® Abstract published in *Advance ACS Abstracts,* March 15, 1995.

0006-2960/95/0434-4402$09.00/0

et al., 1989). In humans, this family includes the *CFTR* chloride channel in which mutations cause cystic fibrosis (Riordan et al., 1989), and the *TAP1/TAP2* heterodimer which actively transports antigenic peptides across the endoplasmic reticulum membrane for association with class I molecules and surface antigen presentation (Trowsdale et al., 1990; Spies et al., 1990).

The 6 TM domains/1 NB site unit may underlie a structural or functional aspect of transport common to these proteins. Clarifying the topology of the membrane-associated domains of these transporters is an important first step for understanding the underlying mechanism of transport. In prokaryotes, genetic analyses of truncated proteins fused to indicator genes (*PhoA*, *LacZ*, *Bla*) have been used to derive structural information on TM regions. Although the 6 or 12 TM domain configuration predicted by hydropathy analysis has been verified in the case of the OppB/OppC (Pearce et al., 1992) and ArsA proteins (Wu et al., 1992), respectively, a similar analysis of HisQ and HisM suggested a 5 TM domain arrangement (Kerppola & Ames, 1992). Analysis of HlyB fusions (Wang et al., 1991) has suggested an 8 rather than a 6 TM domain configuration for HlyB, while other studies were consistent with a 6 TM domain model (Gentschev & Goebel, 1992). Finally, insertion of signals for N-linked glycosylation in discrete segments of CFTR and analysis of the glycosylation profile of the mature proteins have been used to predict extracellular (accessible) and intracellular loops (inaccessible) (Chang et al., 1994). Results from this study confirm the 12 TM domain configuration originally predicted by hydropathy analysis.

Epitope mapping with sequence-specific antibodies has been used to verify certain topological features of P-gp. The cytoplasmic localization of the two ATP-binding domains has been demonstrated in permeabilized cells (Kartner et al., 1985; Yoshimura et al., 1989), and the first predicted extracellular loop has been confirmed to be extracellular, since it is glycosylated (Bruggemann et al., 1989; Schinkel et al., 1993) and is recognized by the antibody MRK-16 in intact cells (Georges et al., 1993). However, studies on the number and topology of the predicted TM domains have yielded contradictory results. Analyses of truncated P-gp molecules translated *in vitro* and translocated into microsomes have suggested that each P-gp half is composed of 4 rather than the predicted 6 TM domains (Zhang & Ling, 1991; Zhang et al., 1993). Expression studies in *Xenopus* oocytes using truncated P-gp fused to a reporter gene have suggested a 6 TM topology for the N-terminal half and a 4 TM configuration for the C-terminal half (Skach et al., 1993; Skach & Lingappa, 1993, 1994). Finally, the elegant analysis of the membrane polarity of P-gp/PhoA fusions expressed in *E. coli* has suggested a 6 TM domain configuration for the N-terminal half of P-gp, although positioning of TM4 was different from that predicted by hydropathy (Bibi & Béjà, 1994).

The discrepancy observed among studies on the membrane topology of P-gp might be linked to the fact that truncated proteins were studied. In addition, results obtained in *in vitro* systems may provide an incomplete picture of the native conformation of the full-length protein in mammalian cells. We have used an alternative but complementary approach to study the topology of the TM domain regions of P-gp. This approach is based on (1) the insertion of an antigenic tag at defined locations in P-gp, (2) the expression of the full-length tagged protein in mammalian cells where its biological activity and integrity can be established, and (3) identifying the location of the epitope tag in intact or permeabilized cells by immunofluorescence and confocal microscopy using a specific antibody directed against the tag. Therefore, in contrast to previous methods, this assay is performed in intact cells with a full-length functional protein. We have recently used this approach to map the membrane topology of the α subunit of the mammalian Na/K-ATPase (Canfield & Levenson, 1993).

EXPERIMENTAL PROCEDURES

Materials. Genetycin (G418) was obtained from Gibco BRL Life Technology Inc. (Burlington, Ontario), vinblastine and colchicine were from Sigma Chemical Co. (St. Louis, MO), and adriamycin and actinomycin-D were a generous gift of Dr. C. Shustik (Royal Victoria Hospital, Montreal, Quebec). All restriction enzymes were obtained from New England Biolabs Ltd. (Mississauga, Ontario) or Pharmacia Biotech Inc. (Baie d'Urfe, Quebec), and were used in buffers and under conditions recommended by the suppliers. The protein assay was from Bio-Rad Laboratories Ltd. (Mississauga, Ontario), the oligonucleotide-directed *in vitro* mutagenesis system (version 2.1, RPN 1523) was from Amersham Canada (Oakville, Ontario), and the monoclonal anti-hemagglutinin (HA) antibody 12CA5 was purchased from Babco Labs (Richmond, CA).

Site-Directed Mutagenesis. Hemagglutinin (HA) epitope tags were introduced into P-gp encoded by the mouse *mdr3* gene as discrete 13 amino acid peptides by site-directed mutagenesis of the mouse *mdr3* cDNA. This HA tag contained the nine amino acids (YPYDVPDYA) derived from influenza virus hemagglutinin A protein, and also the cleavage sequence of factor Xa (IEGR sequence). Full-length cDNA for *mdr3* cloned into the plasmid pGEM7Zf (Promega) was digested with *Sph*I (Polylinker) and *Sma*I (nucleotide position 1767), and the resulting 1.7 kb fragment corresponding to the amino-terminal half of the protein was cloned into the corresponding sites of the plasmid vector M13mp19. The sites of insertions in the Mdr3 protein are shown in relation to calculated hydropathy and predicted TM domains in Figure 1B,C. Novel and unique restriction sites were introduced by the mutant oligonucleotides immediately N-terminal to the inserted HA sequence to facilitate mapping. For this, one or two amino acid residues were replaced by conservative substitutions at the following positions: Phe-Ala at position 100/101 was changed to Tyr-Val, Val to Ile (position 161), Thr to Ser (position 205), Ala to Val (position 244), and Lys to Arg (position 320 and 376). Mutant oligonucleotides (68-72mers, shown in Figure 1D) were annealed to single-stranded M13mp19 DNA templates containing the *mdr3* cDNA fragment, and mutagenesis was carried out using the reagents and procedures of a commercially available *in vitro* system (Amersham, version 2.1, RPN 1523). Insertion of the tag by mutagenesis was monitored by the appearance of novel restriction sites in the cDNA, and the integrity of the entire mutated cDNA inserts was verified by nucleotide sequencing using the dideoxy chain termination method of Sanger et al. (1977). The mutated cDNA inserts were then reconstructed back into the full *mdr3* cDNA in plasmid pGEM7Zf.

Cell Cultures. Wild-type and mutant *mdr3* cDNAs were released from pGEM7Zf by *Kpn*I and *Cla*I digestion and

cloned into the corresponding sites (polylinker) of the mammalian expression vector pCB6 (Canfield & Levenson, 1993), which uses the promotor and enhancer elements of human cytomegalovirus to direct high-level expression of cloned cDNAs. This vector possesses a neomycin resistance gene (*Tn5* transposon) that allows selection of transfected cell clones in genetycin (G418). Drug-sensitive Chinese hamster LR73 ovary cells (Pollard & Stanners, 1979) were transfected by the calcium phosphate precipitation method and grown in α-minimal essential medium (MEM) supplemented with 10% fetal calf serum, 2 mM glutamine, penicillin (50 units/mL), and streptomycin (50 mg/mL). Two days later, cell cultures were split 1:5, and stable transfectants were further selected in the same medium containing G418 (final concentration 500 μg/mL). Pools of multidrug-resistant clones were selected from G418 mass populations by subculture in medium containing vinblastine (final concentration 50 ng/mL).

Membrane Preparation and Western Blotting. Crude membrane fractions of transfected LR73 cells were isolated as described (Devault & Gros, 1990). Briefly, cells grown to 70% confluency were harvested in cold PBS (phosphate-buffered saline) containing citrate, and homogenized in 1 mM $MgCl_2$ and 10 mM Tris, pH 7.0 supplemented with the protease inhibitors leupeptin (2 μg/mL), aprotinin (2 μg/mL), and pepstatin (1 μg/mL) (Dounce homogenizer, 25 strokes up and down). Unbroken cells and nuclei were removed by centrifugation (400 g/10 min) followed by isolation of a crude membrane fraction by centrifugation of the supernatant at 100000*g* for 30 min. Protein concentration was determined by the method of Bradford using a commercially available reagent (Bio-Rad). Proteins (5 μg/lane) were separated on an SDS-containing 7.5% polyacrylamide gel and transferred by electroblotting to nitrocellulose membranes. The nitrocellulose membrane was incubated with the anti-Mdr3-specific rabbit polyclonal antibody B2037 used at a dilution of 1:200 (Devault & Gros, 1990), and immunocomplexes were detected by using a goat anti-rabbit antibody (1:3000) coupled to alkaline phosphatase (Amersham).

Cytotoxicity Assay. Drug cytotoxicity assays were performed according to a method based on the staining of cellular proteins by sulforhodamine B, as previously described (Tang-Wai & Gros, 1993). Briefly, 7.5×10^3 transfected cells or drug-sensitive LR73 control cells were plated in 96-well titer plates in α-MEM medium containing increasing concentrations of either vinblastine, adriamycin, actinomycin-D, or colchicine. The cells were incubated at 37 °C for 72 h and fixed in 17% trichloroacetic acid in PBS, and cellular protein was stained for 10 min at room temperature in 0.4% sulforhodamine B in 1% acetic acid. The plates were then dried, and the stain was dissolved in 0.2 mL of 10 mM Tris (pH 9). Quantification was done using an automated ELISA plate reader (Bio-Rad Model 450) at a wavelength of 490 nm. The relative plating efficiency of each clone was determined by dividing the absorbance observed at a given drug concentration by the absorbance detected in the same clone in medium without drug. The IC_{50} (inhibitory concentration of 50%) is defined as the drug concentration required to reduce the plating efficiency of each clone by 50%. The fold resistance is calculated by dividing the IC_{50} of a given clone by the IC_{50} measured for the drug-sensitive control LR73 cells.

Immunofluorescence and Confocal Microscopy. Localization of the epitope was performed by immunofluorescence and confocal microscopy according to Canfield and Levenson (1993). Transfected LR73 cells, selected in vinblastine at a concentration of 50 ng/mL, and nontransfected cells were grown on glass coverslips. Nonpermeabilized LR73 cells were incubated with the monoclonal antibody 12CA5 (1:500) in Dulbecco minimum essential medium supplemented with 10% FCS and 20 mM Hepes, pH 7.4, for 1 h at 4 °C. This antibody recognizes the inserted epitope YPYDVPDYA (Niman et al., 1983). The cells were fixed in 4% paraformaldehyde in PBS and permeabilized and blocked with 0.05% Nonidet-P40 in PBS, 5% goat serum, and 1% bovine serum albumin at room temperature for 15 min. A secondary antibody (Texas Red-conjugated rabbit anti-mouse IgG; Fisher Scientific) was then applied in the same buffer (dilution of 1:200). In experiments with permeabilized cells, the cells were fixed, permeabilized, and blocked as described above, and then incubated with the first antibody prior to exposure to the second antibody. Immunofluorescence microscopy was performed using standard epifluorescence optics (Zeiss Axiophot) or by confocal laser scanning microscopy using a Bio-Rad MRC 600 confocal microscope (GHS filter block, 514 nm excitation wavelength). Single images were midcell, typically 3−5 μm above coverslip.

RESULTS

Construction of Epitope-Tagged mdr3 cDNAs and Expression in CHO Cells. Hydropathy analysis of P-gp predicts two hydrophobic regions (positions 51−345; 707−990) comprising six transmembrane (TM) domains each, and two hydrophilic domains (positions 346−706; 991−1276), containing the predicted cytoplasmic ATP-binding folds. The aim of the present study was to determine the number and to map the topology of the TM domains in the amino-terminal half of P-gp (mouse *mdr3*). In this segment, combined hydropathy analysis of the three mouse P-gps (Devault & Gros, 1990) predicts TM domains at positions 51−71 (TM1), 116−137 (TM2), 186−205 (TM3), 210−229 (TM4), 293−312 (TM5), and 327−345 (TM6), possibly forming three extracellular and two intracellular loops. We inserted single epitope tags of sequence YPYDVPDYA (hemagglutinin A of influenza virus) in each predicted extracellular and intracellular loop (Figure 1B,C). The introduced epitopes also contained a consensus signal for factor Xa cleavage (IEGR; Consler et al., 1993). The epitope tags were inserted, whenever possible, within regions that were not precisely conserved among the three mouse and two human P-gp isoforms. This was done to minimize the risk of inserting the tag in a key structural/functional domain of the protein, resulting in an inactive mutant. The epitope tags were inserted within the first, second, and third predicted extracellular loops at amino acid positions 101, 206, and 320, respectively, in the first and second predicted intracellular loops at amino acid positions 161, and 244, respectively and near the first ATP-binding site at amino acid position 376 (Figure 1C,D).

Wild-type control and mutant *mdr3* cDNAs corresponding to tagged proteins (numbered 1−6) were inserted into the mammalian expression vector pCB6 and introduced by transfection in drug-sensitive LR73 cells. Stable transfectants were first selected in G418, and multidrug-resistant colonies were further selected in the MDR drug vinblastine (50 ng/

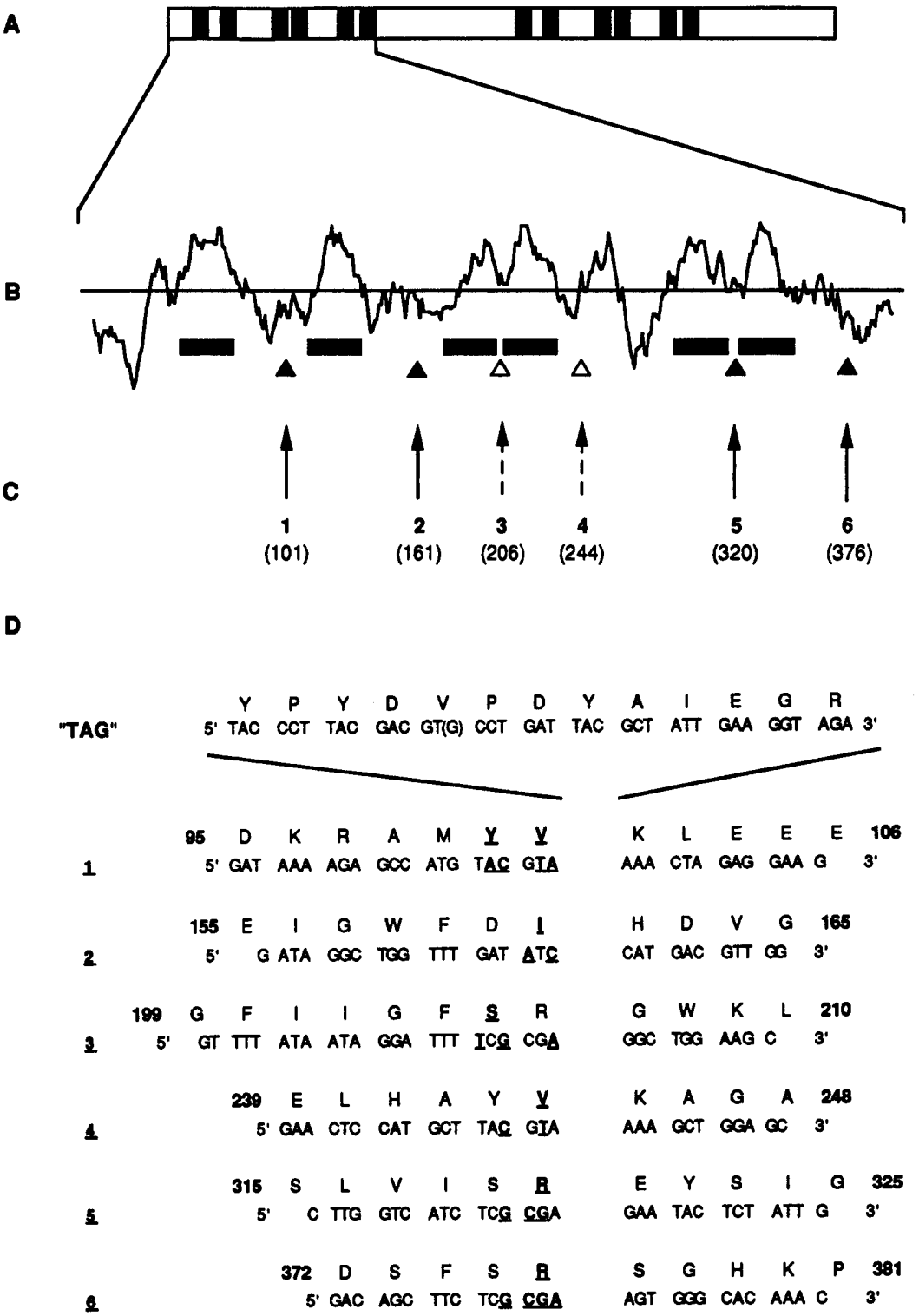

FIGURE 1: Construction of fusion *mdr3* proteins containing HA epitope tags. (A) Schematic representation of the *mdr3* cDNA, including predicted structural domains of the corresponding P-gp. (B) Hydropathy analysis of P-gp encoded by mouse *mdr3* (amino acids 1−400). The average local hydrophobicity at each residue was calculated by the algorithm of Kyte and Doolittle (1982), and the predicted TM domains are identified as dark boxes. (C) Location of the hemagglutinin A (HA) epitope tag onto the secondary structure of P-gp proposed by hydropathy analysis. The fusion proteins are identified as 1−6, with the amino acid residue targeted for HA tag insertion identified in parentheses. Solid arrows and triangles indicate epitope-tagged constructs capable of conferring drug resistance, whereas dashed arrows and white triangles denote epitope-tagged constructs which do not confer drug resistance. (D) Oligonucleotides used for mutagenesis. The nucleotide and translated amino acid sequence of the tag common to all constructs is shown ("TAG"). The sequences flanking the tag on either side are shown for each mutant oligonucleotide (antisense) along with the corresponding amino acid position in the P-gp sequence at the site of insertion. Boldface, underlined characters identify mutated nucleotides, and the resulting amino acids. The corresponding fusion constructs are indicated by boldface, underlined numbers to the left of the panel. In constructs **6**, the nucleotide (G) of the Val codon in the epitope tag was changed to (T) to avoid detrimental secondary structure.

mL). While no drug-resistant colonies could be detected in cells transfected with pCB6 alone after a 3 week selection period, drug-resistant colonies rapidly emerged in cells transfected with wild-type *mdr3*, and this within 5 days of

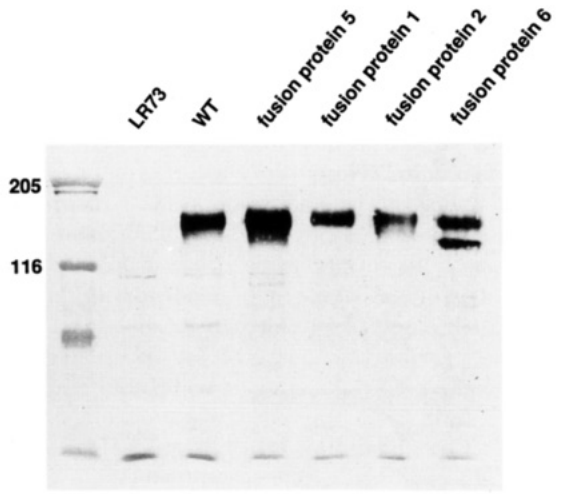

FIGURE 2: Immunoblotting of mouse *mdr3* fusion proteins 1, 2, 5, and 6 expressed in stably transfected cell clones. LR73 hamster ovary cells were transfected with either wild-type or mutant *mdr3* cDNAs containing inserted HA epitopes, and selected in drug-containing medium. Crude membrane fractions were isolated from mass populations of transfected cells. Proteins (5 μg/lane) were resolved on 7.5% SDS−PAGE, and analyzed by immunoblotting with the isoform-specific anti-Mdr3 polyclonal antibody B2037. The position of the molecular mass markers (in kDa) is shown to the left of the figure.

selection. Transfectants of mutant *mdr3* cDNA constructs corresponding to fusion proteins 1, 2, 5, and 6 developed vinblastine-resistant colonies in drug selection either at a high frequency similar to that observed with wild-type *mdr3* (fusion proteins 1, 2, and 5) or at a lower frequency (construct 6). These results indicate that insertion of the epitope tags in these P-gps did not disrupt their capacity to confer drug resistance. On the other hand, cells transfected with mutant *mdr3* cDNA constructs corresponding to fusion proteins 3 and 4 failed to yield drug-resistant colonies even upon reducing the stringency of the drug selection (vinblastine, 25 ng/mL). Since mutations near or within TM domains of P-gp have been shown to alter drug specificity (Gros et al., 1991; Devine et al., 1992; Loo & Clarke, 1993a,b), selection of drug-resistant colonies from constructs 3 and 4 was also attempted in other MDR drugs, adriamycin, colchicine, and actinomycin-D. Such selection also failed to yield drug-resistant colonies. These results indicate that epitope insertions at amino acid positions 206 or 244 are not tolerated to maintain P-gp function, possibly due to alterations in protein folding, membrane targeting, or drug-binding sites.

Crude membrane fractions prepared from mass populations of vinblastine-resistant colonies transfected with constructs 1, 2, 5, and 6 were analyzed for P-gp expression by immunoblotting with an Mdr3 isoform-specific polyclonal rabbit antibody, B2037 (Devault & Gros, 1990). Results in Figure 2 show the presence of a specific immunoreactive band of molecular mass 160 kDa in membrane extracts from the four transfected groups which is absent in nontransfected LR73 control cells. Taken together, these results confirm that fusion proteins 1, 2, 5, and 6 are functional and present within the membrane-enriched fraction of transfected cells. Interestingly, an additional immunoreactive species of molecular mass ~140 kDa was detected in membranes from cell populations expressing fusion protein 6. This band did not appear to be an artifactual degradation P-gp product as it was consistently detected in independent membrane preparations from these cells (data not shown). It may represent a less mature, partially glycosylated form of P-gp that is perhaps retained in the endoplasmic reticulum or Golgi fractions present in our crude membrane extracts.

Drug Resistance Profiles of Fusion P-Glycoproteins. To determine whether insertion of epitope tags in the various *mdr3* mutant cDNAs had additional, more subtle effects on P-gp function, the drug resistance profiles of mass populations of cell clones expressing the corresponding mutant proteins were established for the MDR drugs vinblastine, actinomycin-D, adriamycin, and colchicine (Figure 3). This was done using a cell cytotoxicity assay, and the drug concentrations required to reduce the plating efficiency of each mass population by 50% (IC_{50}) were calculated. All mass populations displayed identical degrees of resistance to vinblastine indistinguishable from transfectants expressing the wild-type protein. For all the other drugs tested, resistance levels similar to wild-type *mdr3* were observed in cells expressing the mutant proteins 1 (first extracellular loop) and 5 (third predicted extracellular loop) (Figure 3). However, mass populations expressing mutant protein 2 (predicted first intracellular loop) displayed lower levels of resistance compared to wild-type *mdr3* in colchicine (*mdr3*, fold resistance 43×; mutant protein 2, 17×), in adriamycin (*mdr3*, 31×; mutant protein 2, 12×), and in particular actinomycin-D (*mdr3*, 44×; mutant protein 2, 6×). A small and less significant decrease in drug resistance was also noted in mass populations expressing mutant protein 6 (Figure 3). Therefore, addition of an epitope at amino acid positions 161 and 376 had a small but noticeable effect on the drug resistance profiles encoded by P-gp. Nevertheless, the preliminary analysis of membrane association (Figure 2) and drug resistance profiles encoded by mutant proteins 1, 2, 5, and 6 (Figure 3) indicate that they are expressed in a functional state in these cells, with only minor alterations in their characteristics.

Localization of the Epitope Tags. The membrane polarity of the epitope tags (inside vs outside) was determined by immunofluorescence on mass populations of stably transfected cells selected in vinblastine. Epitope tags were detected using the mouse anti-HA monoclonal antibody 12CA5 (Niman et al., 1983). The polarity of the tag with respect to its intracellular vs extracellular localization was determined by immunofluorescence either on intact cells (outside) or on cells permeabilized with NP-40 (inside). Representative examples of cells expressing each mutant P-gp analyzed by this method are shown in Figure 4. In intact nontransfected cells (control; Figure 4A,B) and in cells expressing the wild-type Mdr3 protein (nontagged; data not shown), no significant cell-associated fluorescence could be detected either in intact or in permeabilized cells. In contrast, in cells expressing mutant proteins 1 (first predicted extracellular loop) and 5 (third predicted extracellular loop), a strong fluorescent signal was detected in both permeabilized (Figure 4D,H) and intact cells (Figure 4C,G), demonstrating the extracellular localization of the 12CA5 reactive epitope in these fusion proteins. On the other hand, examination of cells expressing mutant proteins 2 (first intracellular loop) or 6 (ATP-binding site) revealed bright fluorescence in permeabilized cells (Figure 4F,J), but no signal in intact cells (Figure 4E,I), indicating an intracellular localization of the epitope tags. In cell populations expressing mutant proteins 1, 2, and 5, fluorescence emission in intact and/or permeabilized cells was uniform over the cells, with an enhanced

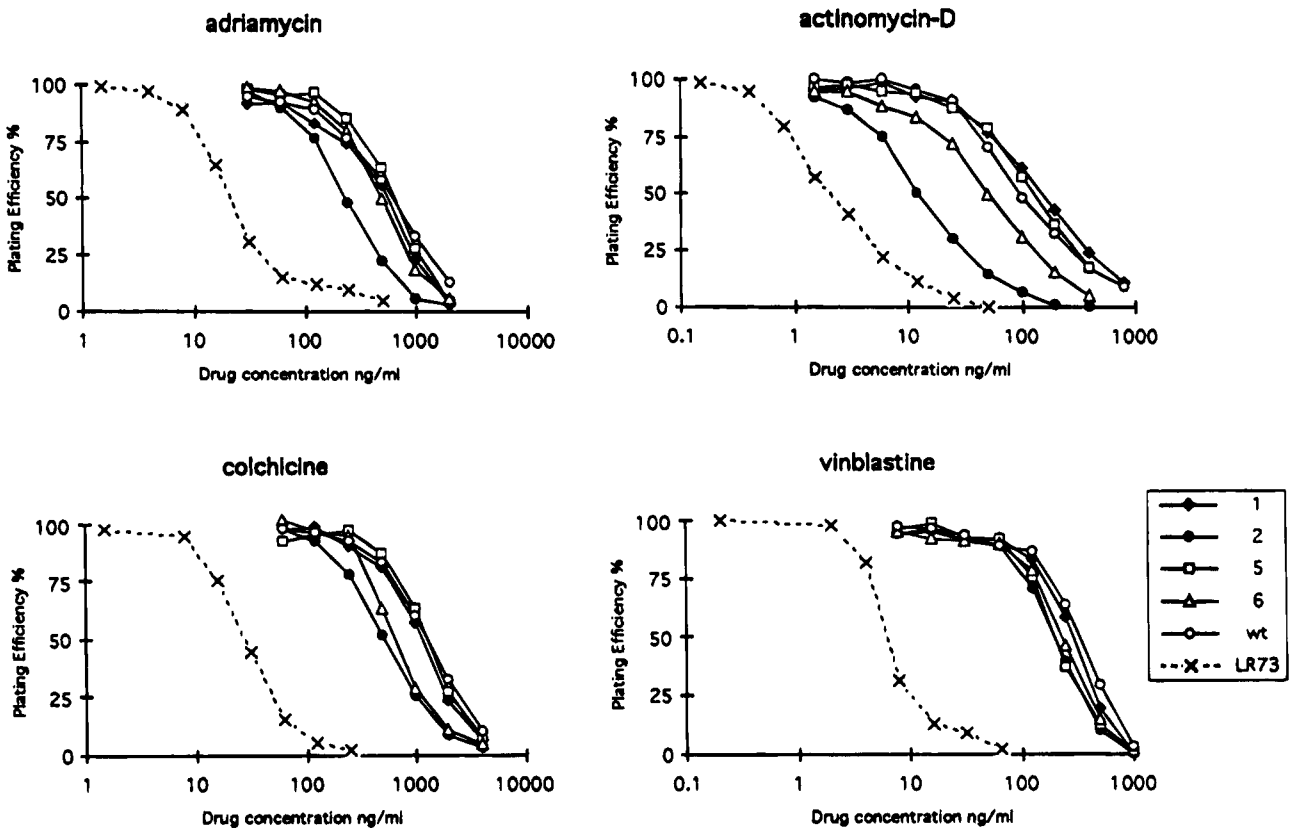

FIGURE 3: Drug survival characteristics of control LR73 cells and drug-resistant *mdr3* transfectants expressing wild-type or fusion proteins 1, 2, 5, and 6. Control drug-sensitive LR73 cells (×, dashed line) and mass populations of cell clones expressing either wild-type Mdr3 (○) or fusion Mdr3 constructs 1 (♦), 2 (●), 5 (□), and 6 (△) were plated in increasing concentrations of either vinblastine, colchicine, adriamycin, or actinomycin-D and further incubated for 72 h. Drug cytotoxicity was measured using a sulforhodamine B staining procedure (Experimental Procedures). The relative plating efficiency of each cell population was calculated by dividing the absorbance measured at a given drug concentration by the value obtained for the same clone in the absence of drug, and was expressed as a percentage (%). Each point represents the average of four independent experiments performed in duplicate dishes.

signal at the edge of the cell, suggestive of membrane association of the tagged proteins. A very small proportion of the fluorescence signal was also observed in some cells in the perinuclear area. In contrast, cells expressing mutant protein 6 were heterogeneous with respect to their staining pattern, with a proportion of cells showing bright staining over the cell surface and at the cell border in permeabilized cells, while other cells also showed a bright perinuclear staining (Figure 4J). These observations suggest that some proportion of construct 6 may be localized in an intracellular compartment.

Confocal microscopy was used to determine more precisely the subcellular distribution of the various mutant proteins. Results of these studies for mutant proteins 2, 6 (both intracellular), and 5 (extracellular) are shown in Figure 5. Confocal microscopy of transfected cells expressing mutant protein 5 revealed a bright fluorescence signal at the cell periphery of intact cells, in a ringlike pattern typical for plasma membrane location (Figure 5A). The analysis of transfected cells stably expressing mutant protein 2 showed a fluorescence signal very similar to that produced by mutant protein 5, indicating an association of the two proteins with the plasma membrane (Figure 5C). For mutant protein 2, a small fraction of the fluorescence signal was also detected in an intracellular location. Permeabilized cells expressing mutant protein 6 revealed both a plasma membrane-associated labeling and also substantial intracellular emission suggested by the width of the ringlike signal in these cells (Figure 5B). Independent analysis of additional cells by confocal microscopy also identified a second population of cells with stronger intracellular staining (data not shown). Although these results are clearly consistent with a plasma membrane location of the majority of the protein, they also suggest that some of the protein is not fully processed in these cells, and is perhaps associated with intracellular organelles such as the Golgi apparatus or endoplasmic reticulum. Interestingly, Western blot analysis of crude membrane extracts from transfectants expressing fusion protein 6 showed not only a ~160 kDa mature protein but also a smaller ~140 kDa protein possibly indicative of incomplete posttranslational modification of this mutant protein (Figure 2). It is tempting to speculate that this incompletely processed mutant P-gp corresponds to the intracellular staining seen by confocal microscopy in cells expressing this protein. Nevertheless, confocal microscopy analysis of these cell clones demonstrates that the vast majority of the fluorescence seen in cells expressing mutant proteins 2, 5, and 6 originates from the plasma membrane, indicative of proper targeting and insertion of the mutant proteins.

DISCUSSION

The elucidation of the three-dimensional structure of a given protein is an important and necessary prerequisite to understand its mechanism of action. The application of standard X-ray crystallography or nuclear magnetic resonance techniques to obtain high-resolution structural information for large integral membrane proteins is difficult, and has been

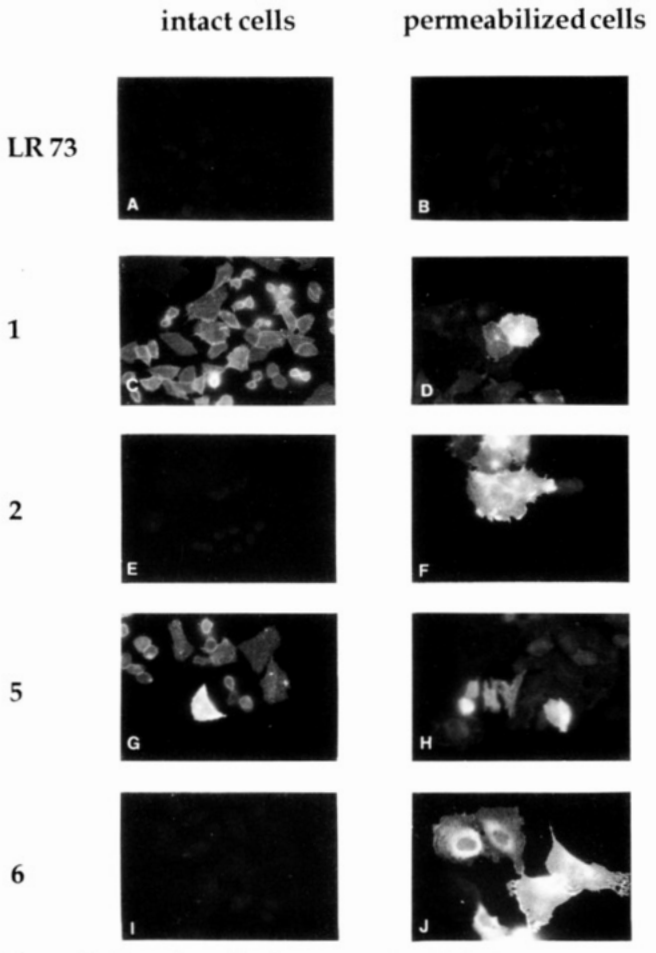

FIGURE 4: Detection of epitope-tagged *mdr3* fusion proteins by immunofluorescence. Control LR73 cells and transfectants stably expressing mutant P-gps 1, 2, 5, and 6 were exposed to the mouse monoclonal anti-HA epitope antibody 12CA5 with (permeabilized cells, right column) or without pretreatment (intact cells, left column) with 0.05% NP-40. Cells were then incubated with a second rabbit anti-mouse antibody conjugated to Texas Red, and the cells were photographed using a fluorescence microscope. The HA epitopes in constructs 2 (E, F) and 6 (I, J) were only detected in permeabilized cells, while the HA epitopes in constructs 1 (C, D) and 5 (G, H) were detected in both permeabilized and nonpermeabilized cells.

successful in only a few cases (Henderson & Unwin, 1975; Deisenhofer et al., 1985; Henderson et al., 1990; Weiss et al., 1991a,b; Cowan et al., 1992). However, considerable information on the two-dimensional structure of membrane proteins can be obtained from the knowledge of their primary amino acid sequence and the application of biochemical, immunological, and genetic analyses. Computer-assisted analysis of the polypeptide sequence using hydropathy plots (Kyte & Doolitle, 1982) or hydrophobic moment (Eisenberg et al., 1984) can be used to predict hydrophobic membrane-spanning domains and provide valuable clues on the membrane topology of these domains. Biochemical, immunological, and genetic methods can then be applied to verify this proposed topology. These include the use of hydrophilic and/or hydrophobic labeling agents that can react with soluble or membrane-bound portions of the proteins (Altenbach et al., 1990), identification of protease-sensitive sites (e.g., Baichwal et al., 1993), epitope mapping with sequence-specific antibodies (Carrasco et al., 1986), or analysis of the polarity of mutant proteins fused to functional marker epitopes [for a review, see Traxler et al. (1993)]. Although the secondary structure prediction and structural models deduced from hydropathy analyses have been proven correct for several integral membrane proteins such as the bacterial lactose permease (Calamia & Manoil, 1990) and the arsenate transporter (Wu et al., 1992), experimental analysis of other membrane proteins such as the bacterial hemolysin transporter (HlyB; Wang et al., 1991) and the mammalian α subunit of the Na/K-ATPase (e.g., Canfield & Levenson, 1993) has revealed discrepancies between the predicted and observed membrane topologies.

Epitope mapping of P-gp using specific antibodies directed against intracellular and extracellular determinants has confirmed the localization of the nucleotide-binding domains (intracellular) and the glycosylated loop (extracellular) (Kartner et al., 1985; Yoshimura et al., 1989; Bruggemann et al., 1989; Georges et al., 1993). However, the exact topology of the two membrane-associated regions of P-gp cannot be addressed by this method, since the size of predicted intra- and extracellular loops is fairly small. Topology mapping of these regions has relied on several alternative approaches such as *in vitro* transcription and translation of truncated polypeptides followed by insertion in microsomes (Zhang & Ling, 1991; Zhang et al., 1993), expression of truncated P-gps linked to a reporter in *Xenopus* oocytes (Skach et al., 1993; Skach & Lingappa, 1993, 1994), and expression of P-gp/alkaline phosphatase (PhoA) fusion proteins in *E. coli* (Bibi & Béjà, 1994). These studies have failed to produce a consistent picture of the topology of P-gp TM regions. The reasons for such discrepancies are not clear, but may be linked to the different experimental systems used and the fact that truncated rather than full-size proteins have been used in these studies. For example, proper insertion of the full-length P-gp into the membrane may require sequence determinants from both the amino and carboxy halves of the protein, and these signals may not be present in truncated proteins. The importance of C-terminal determinants for membrane insertion of segments located more N-terminal has been recently reviewed (Traxler et al., 1993).

We have used a different experimental approach to study the topology of the membrane-associated segments of P-gp. This method relies on the use of an epitope tag (YPYDVPDYA of the hemagglutinin A protein of influenza; HA tag) inserted at strategic locations predicted by hydropathy analysis, and the positions of these tags are then revealed by immunofluorescence in intact cells. We recently have used this approach to map the membrane topology of the α subunit of the mammalian Na/K-ATPase (Canfield & Levenson, 1993). This strategy presents unique advantages over currently used methods. These include the fact that the analyses are carried out (1) on a full-length protein rather than truncated polypeptides, (2) on a functional protein which is capable of conferring multidrug resistance, (3) in whole mammalian cells that can be studied either intact or after membrane permeabilization, and which provide a normal physiological background where proper posttranslational modification can take place (phosphorylation, glycosylation), and (4) using confocal microscopy where the subcellular localization and plasma membrane association can be established unambiguously. We focused our initial studies on the topology of the TM domains in the N-terminal half of P-gp encoded by mouse *mdr3*. A schematic model of the membrane-associated structure of P-gp predicted by hydropathy analysis is shown in Figure 6 [modified from

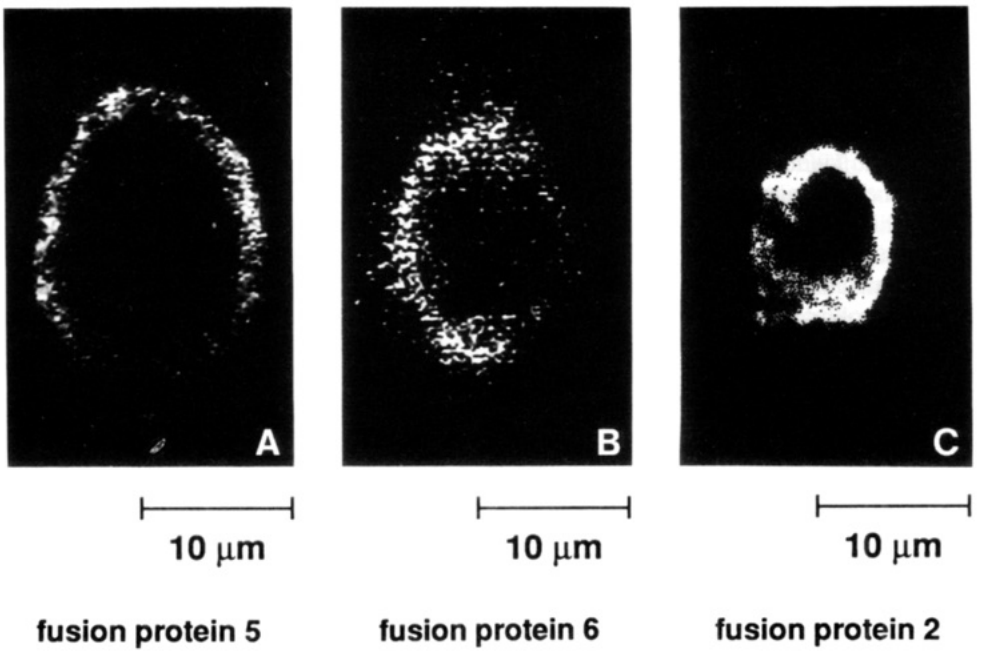

FIGURE 5: Subcellular localization of the epitope-tagged *mdr3* fusion proteins by confocal laser microscopy. Transfected cells stably expressing Mdr3 fusion proteins 2 (C) and 6 (B) were permeabilized, and localization of the tagged proteins was revealed by immunofluorescence with anti-HA antibody 12CA5. Transfected cells expressing fusion protein 5 (A) were analyzed as intact cells. Laser confocal microscopy was done on optical sections scanned through cells at ~3−5 μm above the surface of the coverslip. Scale bar is 10 μm.

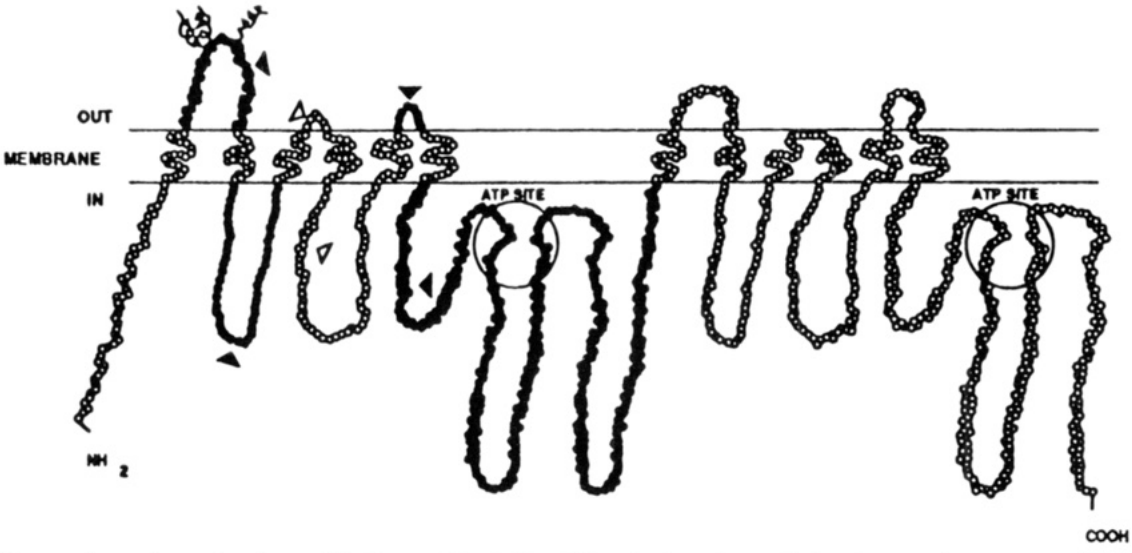

FIGURE 6: Proposed membrane topology of P-glycoprotein deduced from hydropathy analysis. Immunofluorescence with HA epitopes confirmed the extracellular localization of the first and fifth loops of the protein, and the cytoplasmic localization of the second loop and the first ATP-binding site (as indicated by loops with filled circles). NH_2 and COOH indicate the positions of the amino- and carboxyl-terminal ends of the protein. Filled arrowheads indicate the position of HA epitope insertions that resulted in functional P-gps while empty arrowheads indicate the position of HA epitopes which abrogate P-gp function. The position of the nucleotide binding fold is identified by "ATP site". This drawing is a modification of that published by Gottesman and Pastan (1988).

Gottesman and Pastan (1988)]. The method was first tested on one extracellular and one intracellular loop of the protein where the positions with respect to membrane polarity can be inferred from the primary amino acid sequence. The segment delineated by positions 71−116 containing 3 predicted sites for N-linked glycosylation is extracellularly localized, because it is glycosylated and is recognized by antibodies directed against a surface determinant of P-gp (Bruggemann et al., 1989; Schinkel et al., 1993; Georges et al., 1993). Similarly, the ATP-binding sites must be located intracellularly to have access to the ATP substrate, and this has been verified by immunological studies (Kartner et al., 1985; Yoshimura et al., 1989). The analysis of mutant P-gps harboring HA epitope tags within this first predicted extracellular loop (mutant 1) and upstream of the ATP-binding site (mutant 6) indicated that the HA tag insertions at these sites did not alter P-gp function (Figure 3). Results shown in Figures 4 and 5 confirmed their respective locations, as predicted by hydropathy analysis. Similarly insertion of HA tags within segments delineated by amino acid positions 137−186 (mutant 2) and 312−327 (mutant 5) did not disrupt P-gp function, and the mutant P-gps were biologically active and could convey drug resistance (Figure 3). We identified these segments as intracellular and extracellular, respectively.

In addition, careful examination of cells expressing the four biologically active mutant proteins both by normal optics microscopy (Figure 4) and by confocal microscopy (Figure 5) revealed that mutant proteins 1, 2, and 5 were properly targeted to the plasma membrane, and were present at that site in a functional state. A significant part of cells expressing mutant protein 6 showed also clear plasma membrane staining (Figures 4J and 5B). In some cells, however, strong intracellular fluorescence emission was observed in addition to the emission along the plasma membrane, suggesting that a fraction of mutant protein 6 was not properly targeted to the plasma membrane. Thus, the study of mutant P-gps 1, 2, 5, and 6 allowed the unambiguous positioning of two intracellular and two extracellular loops and inferred the presence of at least four TM domains (TM1, TM2, TM5, TM6) in this region.

The positioning of predicted TM domains 3 and 4 was attempted in mutant proteins 3 and 4, in which the HA tag was inserted at positions 206 (predicted extracellular) and 244 (predicted intracellular), respectively. Unfortunately, addition of the HA tag at these sites resulted in nonfunctional proteins that could not be analyzed. In the case of mutant protein 3 (tag position 206), hydropathy analysis predicts that this extracellular loop would be only four amino acid residues in length. Such a short segment may be completely included within the lipid bilayer, and insertions at that site may have deleterious effects on the packing of the adjacent TM domains in the final three-dimensional structural arrangement of the protein, resulting in the loss of function. A possible alternative would be to use an epitope tag smaller than the 13 residue (HA and factor Xa cleavage site) segment used in this study. The lack of activity of P-gp mutant 4 is more difficult to explain on a strictly structural basis with respect to its position relative to TM domains. Indeed, the second predicted intracellular loop in which the HA tag was inserted in hydrophilic and is predicted to be formed by 62 amino acids. However, its sequence is fairly conserved among the various mouse P-gp isoforms, and, therefore, it may play an important role in the mechanism of action of P-gp. Alternatively, this region could be important for proper targeting of the protein to subcellular compartments for posttranslational modifications and trafficking to the membrane. However, it is tempting to speculate that the functional property impaired in this mutant may be related to an important role of intracellular loops in drug binding and/or transport by the protein. Indeed, we noted that although successful insertion of HA tags in the predicted extracellular loops (mutant 1 and 5) had no effect on the substrate specificity of P-gp, insertion of the tags in intracellular loops (mutants 2 and 6) had an effect on the overall drug resistance profiles encoded by the mutant proteins. The parallel biochemical analysis of naturally occurring (Tsui, 1992) or experimentally introduced mutations (Chang et al., 1994) in another member of the superfamily of ABC transporters, the CFTR, suggests that alterations in the predicted intracellular loops of this class of proteins have more deleterious effects on function than similar mutations introduced in predicted extracellular loops, possibly due to impaired maturation of the polypeptide. Insertion of the epitope tag at other amino acid positions within this loop may bypass such a block and produce a functional protein in which the polarity of the loop can be unambiguously established.

In conclusion, epitope tagging proves to be a very useful and complementary method to analyze the topology of the membrane-associated region of P-gp. In addition, the epitope tag insertion protocol has also proven useful to identify regions of the protein in which integrity is absolutely essential for function and that do not tolerate the 13 amino acid insertion. Further scanning with additional epitope insertions should, on the one hand, allow the precise delineation of individual TM domains and, on the other hand, should help further define those discrete regions in the intracellular loops that cannot be altered by epitope insertion without loss of function.

REFERENCES

Abraham, E. H, Prat, A. G., Gerweck, L., Seneveratne, T., Arceci, R. J., Kramer, R., Guidotti, G., & Cantiello, H. F. (1993) *Proc. Natl. Acad. Sci. U.S.A. 90*, 312−316.

Altenbach, C., Marti, T., Khorana, H. G., & Hubbell, W. L. (1990) *Science 248*, 1088−1092.

Baichwal, V., Liu, D., & Ames, G. F.-L. (1993) *Proc. Natl. Acad. Sci. U.S.A. 90*, 620−624.

Bibi, E., & Béjà, O. (1994) *J. Biol. Chem. 269*, 19910−19915.

Bruggemann, E. P., Germann, U. A., Gottesman, M. M., & Pastan, I. (1989) *J. Biol. Chem. 264*, 15483−15488.

Calamia, J., & Manoil, C. (1990) *Proc. Natl. Acad. Sci. U.S.A. 87*, 4937−4941.

Canfield, V. A., & Levenson, R. (1993) *Biochemistry 32*, 13782−13786.

Carrasco, N., Herzlinger, D., Danho, W., & Kaback, H. R. (1986) *Methods Enzymol. 125*, 453−467.

Chang, X.-B., Hou, Y.-X., Jensen, T. J., & Riordan, J. R. (1994) *J. Biol. Chem. 269*, 18572−18575.

Chen, C., Chin, J. E., Ueda, K., Clark, D. P., Pastan, I., Gottesman, M. M., & Roninson, I. B. (1986a) *Cell 47*, 381−389.

Chen, C. M., Misra, T. K., Silver, S., & Rosen, B. P. (1986b) *J. Biol. Chem. 261*, 15030−15038.

Consler, T. G., Persson, B. L., Jung, H., Zen, K. H., Jung, K., Privé, G. G., Verner, G. E., & Kaback, H. R. (1993) *Proc. Natl. Acad. Sci. U.S.A. 90*, 6934−6938.

Cornwell, M. M., Safa, A. R., Felsted, R. L., Gottesman, M. M., & Pastan, I. (1986) *Proc. Natl. Acad. Sci. U.S.A. 83*, 3847−3850.

Cornwell, M. M., Tsuruo, T., Gottesman, M. M., & Pastan, I. (1987) *FASEB J. 1*, 51−54.

Cowan, S. W., Schirmer, T., Rummel, G., Steiert, M., Ghosh, R., Pauptit, R. A., Jansonius, J. N., & Rosenbusch, J. P. (1992) *Nature 358*, 727−733.

Deisenhofer, J., Epp, O., Miki, K., Huber, R., & Michel, H. (1985) *Nature 318*, 618−624.

Devault, A., & Gros, P. (1990) *Mol. Cell. Biol. 10*, 1652−1663.

Devine, S. E., Ling, V., & Melera, P. W. (1992) *Proc. Natl. Acad. Sci. U.S.A. 89*, 4564−4568.

Eisenberg, D., Schwarz, E., Komaromy, M., & Wall, R. (1984) *J. Mol. Biol. 179*, 125−142.

Felmlee, T., Pellett, S., & Welch, R. A. (1985) *J. Bacteriol. 163*, 94−105.

Foote, S. J., Thompson, J. K., Cowman, A. F., & Kemp, D. J. (1989) *Cell 57*, 921−930.

Gentschev, I., & Goebel, W. (1992) *Mol. Gen. Genet. 232*, 40−48.

Georges, E., Tsuruo, T., & Ling, V. (1993) *J. Biol. Chem. 268*, 1792−1798.

Gottesman, M. M., & Pastan, I. (1988) *J. Biol. Chem. 263*, 12163−12166.

Gottesman, M. M., & Pastan, I. (1993) *Annu. Rev. Biochem. 62*, 385−427.

Gros, P., Croop, J., & Housman, D. (1986) *Cell 47*, 371−380.

Gros, P., Raymond, M., Bell, J., & Housman, D. (1988) *Mol. Cell. Biol. 8*, 2770−2778.

Gros, P., Dhir, R., Croop, J., & Talbot, F. (1991) *Proc. Natl. Acad. Sci. U.S.A. 88*, 7289−7293.

Henderson, R., & Unwin, P. N. T. (1975) *Nature 257*, 28−32.

Henderson, R., Baldwin, J. M., Ceska, T. A., Zemlin, F., Beckmann, E., & Downing, K. H. (1990) *J. Mol. Biol. 213*, 899−929.
Higgins, C. F. (1992) *Annu. Rev. Cell Biol. 8*, 67−113.
Kartner, N., Evernden-Porelle, D., Bradley, G., & Ling, V. (1985) *Nature 316*, 820−823.
Kerppola, R. E., & Ames, G. F.-L. (1992) *J. Biol. Chem. 267*, 2329−2336.
Kyte, J., & Doolittle, R. F. (1982) *J. Mol. Biol. 157*, 105−132.
Loo, T. W., & Clarke, D. M. (1993a) *J. Biol. Chem. 268*, 3143−3149.
Loo, T. W., & Clarke, D. M. (1993b) *J. Biol. Chem. 268*, 19965−19972.
McGrath, J. P., & Varshavsky, A. (1989) *Nature 340*, 400−404.
Niman, H. L., Houghten, R. A., Walker, L. E., Reisfeld, R. A., Wilson, I. A., Hogle, J. M., & Lerner, R. A. (1983) *Proc. Natl. Acad. Sci. U.S.A. 80*, 4949−4953.
Pearce, S. R., Mimmack, M. L., Gallagher, M. P., Gileadi, U., Hyde, S. C., & Higgins, C. F. (1992) *Mol. Microbiol. 6*, 47−57.
Pollard, J. W., & Stanners, C. P. (1979) *J. Cell. Physiol. 98*, 571−585.
Riordan, J. R., Rommens, J. M., Kerem, B.-S., Alon, N., Rozmahel, R., Grzelczak, Z., Zielenski, J., Lok, S., Plavsic, N., Chou, J.-L., Drumm, M. L., Iannuzzi, M. C., Collins, F. S., & Tsui, L.-C. (1989) *Science 245*, 1066−1073.
Roepe, P. D., Wei, L. Y., Cruz, J., & Carlson, D. (1993) *Biochemistry 32*, 11042−11056.
Ruetz, S., & Gros, P. (1994) *J. Biol. Chem. 269*, 12277−12284.
Safa, A. R. (1993) *Cancer Invest. 11*, 46−56.
Safa, A. R., Glover, C. J., Meyers, M. B., Biedler, J. L., & Felsted, R. L. (1986) *J. Biol. Chem. 261*, 6137−6140.
Sanger, F., Nicklen, S., & Coulson, A. R. (1977) *Proc. Natl. Acad. Sci. U.S.A. 74*, 5463−5467.
Schinkel, A. H., Roelofs, M. E. M., & Borst, P. (1991) *Cancer Res. 51*, 2628−2635.
Schinkel, A. H., Kemp, S., Dolle, M., Rudenko, G., & Wagenaar, E. (1993) *J. Biol. Chem. 268*, 7474−7481.
Schurr, E., Raymond, M., Bell, J. C., & Gros, P. (1989) *Cancer Res. 49*, 2729−2734.
Shapiro, A. B., & Ling, V. (1994) *J. Biol. Chem. 269*, 3745−3754.
Skach, W. R., & Lingappa, V. R. (1993) *J. Biol. Chem. 268*, 23552−23561.
Skach, W. R., & Lingappa, V. R. (1994) *Cancer Res. 54*, 3202−3209.
Skach, W. R., Calayag, M. C., & Lingappa, V. R. (1993) *J. Biol. Chem. 268*, 6903−6908.
Spies, T., Bresnahan, M., Bahram, S., Arnold, D., Blanck, G., Mellins, E., Pious, D., & De Mars, R. (1990) *Nature 348*, 744−747.
Surin, B. P., Rosenberg, H., & Cox, G. B. (1985) *J. Bacteriol. 161*, 189−198.
Tang-Wai, D. F., Brossi, A., Arnold, L. D., & Gros, P. (1993) *Biochemistry 32*, 6470−6476.
Traxler, B., Boyd, D., & Beckwith, J. (1993) *J. Membr. Biol. 132*, 1−11.
Trowsdale, J., Hanson, I., Mockridge, I., Beck, S., Townsend, A., & Kelly, A. (1990) *Nature 348*, 741−743.
Tsui, L.-C. (1992) *Trends Genet. 8*, 392−398.
Valverde, M. A., Díaz, M., Sepúlveda, F. V., Gill, D. R., Hyde, S. C., & Higgins, C. F. (1992) *Nature 355*, 830−833.
Wang, R., Seror, S. J., Blight, M., Pratt, J. M., Broome-Smith, J. K., & Holland, I. B. (1991) *J. Mol. Biol. 217*, 441−454.
Weiss, M. S., Abele, U., Weckesser, J., Welte, W., Schiltz, E., & Schulz, G. E. (1991a) *Science 254*, 1627−1630.
Weiss, M. S., Kreusch, A., Schiltz, E., Nestel, U., Welte, W., Weckesser, J., & Schulz, G. E. (1991b) *FEBS Lett. 280*, 379−382.
Wu, J., Tisa, L. S., & Rosen, B. P. (1992) *J. Biol. Chem. 267*, 12570−12576.
Yoshimura, A., Kuwazuru, Y., Sumizawa, T., Ichikawa, M., Ikeda, S., Uda, T., & Akiyama, S. (1989) *J. Biol. Chem. 264*, 16282−16291.
Zhang, J.-T., & Ling, V. (1991) *J. Biol. Chem. 266*, 18224−18232.
Zhang, J.-T., Duthie, M., & Ling, V. (1993) *J. Biol. Chem. 268*, 15101−15110.

BI942735K